

The $^{68}\text{Ga}/^{177}\text{Lu}$ theragnostic concept in PSMA targeting of castration-resistant prostate cancer: correlation of SUV_{max} values and absorbed dose estimates

Lorenza Scarpa¹ · Sabine Buxbaum¹ · Dorota Kendler¹ · Katharina Fink^{1,2} · Jasmin Bektic³ · Leonhard Gruber⁴ · Clemens Decristoforo¹ · Christian Uprimny¹ · Peter Lukas² · Wolfgang Horninger³ · Irene Virgolini¹

Received: 31 August 2016 / Accepted: 23 December 2016 / Published online: 12 January 2017
© The Author(s) 2017. This article is published with open access at Springerlink.com

Abstract

Introduction A targeted theragnostic approach based on increased expression of prostate-specific membrane antigen (PSMA) on PC cells is an attractive treatment option for patients with metastatic castration-resistant prostate cancer (mCRPC).

Methods Ten consecutive mCRPC patients were selected for ^{177}Lu -PSMA617 therapy on the basis of PSMA-targeted ^{68}Ga -PSMA-HBED-CC PET/CT diagnosis showing extensive and progressive tumour load. Following dosimetry along with the first therapy cycle restaging (^{68}Ga -PSMA-HBED-CC and ^{18}F -NaF PET/CT) was performed after 2 and 3 therapy cycles (each 6.1 ± 0.3 GBq, range 5.4–6.5 GBq) given intravenously over 30 minutes, 9 ± 1 weeks apart. PET/CT scans were compared to ^{177}Lu -PSMA617 24-hour whole-body scans and contrast-enhanced dual-phase CT. Detailed comparison of SUV_{max} values and absorbed tumour doses was performed.

Results ^{177}Lu -PSMA617 dosimetry indicated high tumour doses for skeletal (3.4 ± 1.9 Gy/GBq; range 1.1–7.2 Gy/GBq), lymph node (2.6 ± 0.4 Gy/GBq; range 2.3–2.9 Gy/GBq) as well as liver (2.4 ± 0.8 Gy/GBq; range 1.7–3.3 Gy/GBq) metastases whereas the dose for tissues/organs was acceptable in all patients for an intention-to-treat activity of 18 ± 0.3 GBq. Three patients showed partial remission, three mixed response, one stable and three progressive disease. Decreased ^{177}Lu -PSMA617 and ^{68}Ga -PSMA-HBED-CC uptake (mean SUV_{max} values 20.2 before and 15.0 after 2 cycles and 11.5 after 3 cycles, $p < 0.05$) was found in 41/54 skeletal lesions, 12/13 lymph node metastases, 3/5 visceral metastases and 4/4 primary PC lesions.

Conclusion Due to substantial individual variance, dosimetry is mandatory for a patient-specific approach following ^{177}Lu -PSMA617 therapy. Higher activities and/or shorter treatment intervals should be applied in a larger prospective study.

Keywords $^{68}\text{Ga}/^{177}\text{Lu}$ PSMA-targeted theragnostic concept · Prostate cancer · ^{18}F -NaF-PET · Dosimetry

Electronic supplementary material The online version of this article (doi:10.1007/s00259-016-3609-9) contains supplementary material, which is available to authorized users.

✉ Irene Virgolini
irene.virgolini@i-med.ac.at; <http://nuklearmedizin-innsbruck.com>

¹ Department of Nuclear Medicine, Medical University Innsbruck, Anichstraße 35, A-6020 Innsbruck, Austria

² Department of Radiotherapy / Radiation Oncology, Medical University of Innsbruck, Innsbruck, Austria

³ Department of Urology, Medical University of Innsbruck, Innsbruck, Austria

⁴ Department of Radiology, Medical University of Innsbruck, Innsbruck, Austria

Introduction

Despite the high incidence of prostate cancer (PC), the 5-year survival rate is almost 100% if the disease is localized [1]. However, when PC has spread beyond the gland, the mortality rate increases dramatically and in advanced stages, PC becomes the third most frequent cause of cancer-related mortality in men [1]. Biochemical relapse (BR) is seen in about 25% after radical prostatectomy (RP), and in around 60% of PC patients after primary external beam radiotherapy (EBRT) [2]. Based on the increased expression of prostate-specific membrane antigen (PSMA) on PC cells, various radioligands have been clinically

used to localize or detect PC lesions [3–8]. We have recently shown that the prostate-specific antigen (PSA) level and the PSA doubling time are valuable predictors of pathological PET/CT findings using ^{68}Ga -(Glu-NH-CO-NH-Lys-(Ahx)-[^{68}Ga (HBED-CC)]) as radioligand [6]. Most importantly, this new imaging modality revealed a higher probability for a positive PET finding in patients with low PSA values (<0.5 ng/ml) than any other imaging modality, which can substantially influence the clinical management. Furthermore, a higher detection rate and higher tumour-to-background ratio for PC lesions was reported for PSMA-targeted PET/CT as compared to ^{18}F -Cholin PET/CT [9]. PET/CT with a PSMA-targeting radioligand may also be superior to ^{18}NaF PET/CT for the evaluation of response to ^{223}Ra -chloride therapy in PC patients with bone metastases [10].

Initially, almost all patients with hormone-naïve PC have a good response to the well-established anti-androgen treatments. Over the last several years, even for patients with metastatic castration-resistant prostate cancer (mCRPC), significant improvements were observed following treatment with the androgen receptor antagonist enzalutamide or the CYP17A1 inhibitor abiraterone [11]. However, resistance to these treatments occurs frequently within 1 to 2 years. For this reason, a targeted radionuclide approach could be an attractive and quickly developing therapy option. The PSMA expression of PC cells is directly correlated to androgen independence, metastasis formation and PC progression [12]. Therefore, the PSMA-targeting theragnostic concept potentially offers advantages in regard to diagnosis but also the therapy of mCRPC patients, if labelled with ^{177}Lu [13–19], ^{131}I [4], auger [20] or an alpha-emitting isotope [21].

In this study, we report the dosimetric data and clinical results of 10 consecutive mCRPC patients treated with ^{177}Lu -PSMA617 and followed up by ^{68}Ga -PSMA-HBED-CC and ^{18}F -NaF PET/CT.

Materials and methods

Ethical and regulatory issues

The application of ^{177}Lu -PSMA617 was approved by the institutional review tumour board and all patients gave written informed consent to therapy and imaging studies. All patients received ^{177}Lu -PSMA617 under compassionate use condition according to the updated Declaration of Helsinki [22], prepared according to the Austrian Medicinal Products Act, AMG § 8a [23]. All patients were informed about the experimental nature of the ^{177}Lu -PSMA617 therapy and no systematic patient selection was performed. All regulations of the Austrian Agency for Radiation Protection were observed [24].

Patient selection

Ten patients (range 56–82 years) with progressive mCRPC (mean age 68 years, Gleason score ≥ 8) were prospectively assigned to undergo ^{177}Lu -PSMA617 therapy with 3 cycles (each 6 GBq) applied 8 to 10 weeks apart.

^{177}Lu -PSMA617 was offered as surrogate therapy to patients who were refractory to chemotherapy, monoclonal antibody therapy and/or hormonal therapy as indicated in Table 1. Three patients were pre-treated with ^{223}Ra -chloride and the other three patients with zoledronic acid. Patients were selected on the basis of progressive mCRPC diagnosis based on ^{68}Ga -PSMA-HBED-CC PET/CT imaging.

Preparation of radiolabeled PSMA-targeting ligands

The GMP precursors DOTA-PSMA617 and PSMA-HBED-CC were obtained from Advanced Biochemical Compounds (ABX, Radeberg, Germany), n.c.a. ^{177}Lu -chloride from Isotope Technologies Garching GmbH (ITG, Garching, Germany), and ^{68}Ga -chloride was obtained by elution of a $^{68}\text{Ge}/^{68}\text{Ga}$ generator (IGG100; Eckert & Ziegler, Berlin; 1.850 MBq reference activity) with 6 ml 0.1 N HCl.

Preparation of ^{177}Lu -PSMA617

^{177}Lu -DOTA-PSMA617 was prepared using a fully automated synthesis module based on single-use cassettes (PharmTracer, Eckert&Ziegler) in analogy to the preparation of ^{177}Lu -somatostatin analogues as previously described [25]. Reaction was performed in a sodium ascorbate buffer with a pH of 4.5, 15 minutes heating at 90 °C and 60 MBq $^{177}\text{Lu}/\mu\text{g}$ precursor. The reaction solution was purified using a C-18 reversed-phase cartridge (SEPPAK) and sterile-filtered, resulting in almost quantitative (>90%) yields and high radiochemical purity (>92%, <1% free ^{177}Lu) as determined by reversed-phase HPLC using an isocratic TFA/acetonitrile/water gradient and TLC. Additionally, precursor amount half-life, appearance, pH, ethanol content, sterility and endotoxins were determined.

Preparation of ^{68}Ga -PSMA-HBED-CC

^{68}Ga -PSMA-HBED-CC was prepared as described previously [6] using a fully automated synthesis module based on single-use cassettes (PharmTracer, Eckert&Ziegler). Briefly, ^{68}Ga -chloride was absorbed on an SCX cation exchange cartridge. The activity was eluted from the cartridge with a concentrated NaCl/HCl solution and added to 10 μg ^{68}Ga -PSMA-HBED-CC, 50 μl 0.2 M ascorbic acid and 0.4 ml 2 M sodium acetate buffer, pH 4.5, to a total volume of 1.5 ml. The resulting solution was heated to 95 °C for 10 minutes, purified by SEPPAK and sterile-filtered. Radiochemical purity exceeded 90% with <2% free Ga^{3+} and colloidal ^{68}Ga .

Table 1 Demographic data of metastatic castration-resistant prostate cancer patients

Patient	Age	Previous therapies						
		Surgery	Radiotherapy	Chemotherapy	Monoclonal anti-body	Hormonal therapy	Supportive therapy	²²³ Ra (MBq)
1	75	Prostatectomy Vesiculectomy	External beam radiation therapy	/	/	Degarelix + bicalutamide	Zoledronic acid	/
2	76	Prostatectomy	/	/	/	Leuprorelin	/	/
3	61	/	External beam radiation therapy	Docetaxel	/	Degarelix + bicalutamide + dutasteride; degarelix; enzalutamide + degarelix	/	24.4
4	68	/	/	/	/	Bicalutamide + leuprorelin	/	/
5	63	Prostatectomy	External beam radiation therapy	/	Denosumab	Abiraterone + leuprorelin	/	18.1
6	74	Palliative prostatectomy, decompression 14/15	/	/	/	Goserelin + enzalutamide	Zoledronic acid	/
7	59	Prostatectomy	/	Taxotere	Denosumab	Bicalutamide + tamoxifene; abiraterone; enzalutamide	Zoledronic acid	/
8	56	/	/	Taxotere	Denosumab	Degarelix; pamorelin; leuprorelin	/	26.3
9	66	Prostatectomy Vesiculectomy	/	/	Denosumab	Leuprorelin; pamorelin	/	/
10	82	Prostatectomy	Proton therapy	/	Denosumab	Leuprorelin; enzalutamide	/	/

Administration of ¹⁷⁷Lu-PSMA617 and safety procedures

According to the Austrian radiation protection laws, all patients were treated as in-patients at the nuclear medicine ward and could be discharged 48 hours post injection. Clinical examinations were done prior to therapy and before discharge. Patients received an intravenous hydration (1000 ml 0.9% NaCl, flow 300 ml/h) starting 30 minutes prior to ¹⁷⁷Lu-PSMA617 therapy (flow 100 ml/h, 100 ml) which was administered by a dedicated infusion pump system. After each therapy cycle, blood cell count was determined every 2 weeks. In addition, every 4 weeks renal and liver function parameters as well as PSA were evaluated. Laboratory values were classified into toxicity grades using the Common Terminology Criteria for Adverse Events 3.0 (CTCAE). [26]. All patients were clinically monitored for vital parameters as well as possible side effects (such as xerostomia, nausea, vomiting, pain, tiredness, fatigue, etc.) using the standard hospital monitoring and documentation systems during their residence.

Response assessment

Morphological and functional imaging assessments were done by PET/CT using ⁶⁸Ga-PSMA617 and ¹⁸F-NaF before the first therapy cycle, after 2 cycles (i.e. 18 to 20 weeks) and 8 to 10 weeks after the third therapy cycle (i.e. 24 to 30 weeks after the first therapy cycle). The study evaluation followed an

intention-to-treat approach and patients were followed up until death. PET scans were compared to whole-body scans acquired at 24 hour post-infusion of ¹⁷⁷Lu-PSMA617. For response assessment, we used RECIST criteria and/or lesion size and intensity of uptake [maximum standardized uptake value (SUV_{max})] in metastases in ⁶⁸Ga-PSMA-HBED-CC PET/CT. Progressive disease (PD) was defined by appearance of new lesions and/or increase of uptake, partial remission (PR) by disappearance of one or more lesions and/or decrease of uptake, stable disease (SD) by no changes in number and uptake of the tumour lesions and mixed response (MX) by disappearance and/or decrease of uptake of some lesions next to appearance of new lesions.

⁶⁸Ga-PSMA-HBED-CC PET/CT imaging and SUV_{max} analysis

⁶⁸Ga-PSMA-HBED-CC PET/CT imaging was performed using a dedicated PET/CT system (Discovery 690; GE Healthcare, Milwaukee, WI, USA). An average activity of 145 ± 10 MBq (range 120–160 MBq) ⁶⁸Ga-PSMA-HBED-CC was administered intravenously. In all patients, an attenuation-corrected whole-body scan (skull to mid-thighs) in three-dimensional (3D) mode (emission time 2 minutes with an axial field of view of 15.6 cm per bed position) starting 60 minutes after tracer injection was acquired with an image matrix size of 128 × 128 (pixel size 5.5 mm). In all patients,

either a diagnostic or low-dose CT scan was performed, the latter only for attenuation correction of the PET emission data. The low-dose CT scan parameters using "GE smart mA dose modulation" were: 100 kVp, 50 mA, 0.8 seconds per tube rotation, slice thickness 3.75 mm, and pitch 1.375.

The contrast-enhanced (ce) CT scan parameters using GE smart mA dose modulation were: 100–120 kVp, 120 mA, 0.8 seconds per tube rotation, slice thickness 3.75 mm, and pitch 0.984. A CT scan of the thorax, abdomen and pelvis (shallow breathing) was acquired 40 to 70 seconds after injection of contrast agent (60 to 120 ml of Iomeron [Ultravist®, Bayer Schering Pharma, Berlin, Germany] 370 mg/l, depending on patient body weight). Compared to high-dose ceCT, low-dose CT in this setting was sufficient for anatomical localization and characterization of ^{68}Ga -PSMA-HBED-CC-positive lesions, e.g. lymph node (LN) metastases.

All ^{68}Ga -PSMA-HBED-CC PET/CT images were analysed with dedicated commercially available software (eNTEGRA; GE Healthcare, Milwaukee, WI, USA), which allowed the review of PET, CT and fused imaging data. PET/CT images were interpreted by at least two board-certified nuclear medicine/radiologists with more than 5 years of clinical experience aware of all clinical data available.

Visual interpretation was the main criterion for reaching the final diagnosis. Any uptake higher than surrounding background activity, which did not correlate with physiological tracer uptake, was considered pathological and suspicious for malignancy. In addition, semi-quantitative analysis of all pathological lesions was performed by comparing the SUV_{max} in the 60-minute scan with background activity. All patients had multiple lesions (prostate bed, bone, LNs, liver) which were chosen for SUV_{max} analysis. SUV_{max} calculation was obtained by drawing circular regions of interest (ROIs) using the commercial software provided by the vendor. Several areas of background were selected corresponding to the location of the pathological lesions.

^{18}F -NaF PET/CT imaging

^{18}F -NaF PET/CT (IASOFLU®, IASON GmbH, Austria) was administered at an average activity of 155 ± 44 MBq (range 101 to 250 MBq). After an accumulation phase of 120 minutes, PET imaging was performed using a dedicated PET/CT system (Discovery 690; GE Healthcare, Milwaukee, WI, USA). An attenuation-corrected whole-body scan (skull to base to mid-thighs) in 3D mode (emission time two minutes with an axial field of view of 15.6 cm per bed position) starting 120 minutes after tracer injection was acquired with an image matrix size of 128×128 (pixel size 5.5 mm). In all patients, a low-dose CT scan was performed for attenuation correction of the PET emission data.

^{177}Lu -PSMA617 whole-body imaging and dosimetry calculation

Dosimetry based on the medical internal radiation dose (MIRD) principle was performed following the application of the first ^{177}Lu -PSMA617 therapy cycle. All patients received planar anterior and posterior whole-body-scans with a dual-headed gamma camera (SIEMENS Symbia, Erlangen, Germany). For imaging, a medium-energy parallel whole collimator was used; the scan speed was set to 15 cm/min and a photo-peak window was centered at 208 keV with an energy window of 15%. Scans were performed at 0.5, 4, 24, 72 and 96 hours post-infusion. In addition, SPECT/CT imaging of the abdomen was performed at 24 hours to rule out possible overlays between different organs/tumours and to evaluate organ and tumour volumes. ROIs of tumours and all relevant organs at risk (OARs) were drawn on the 24-hour image using the Hermes software. In addition, a ROI was drawn near the femur and one at the sinus frontalis to establish an appropriate background correction. All ROIs were copied to the other images (0.5, 4, 76 and 96 hours) and the geometric mean of the anterior and posterior projections of the planar image was further analyzed by an Excel script. OLINDA/EXM-based [27] dosimetry was performed according to the information provided in the supplement 1.

Statistics

All results are expressed as mean \pm standard deviation. Wilcoxon's signed rank test was used to compare different groups. A p value lower than 0.05 was considered significant.

Results

Evaluation of ^{177}Lu -PSMA617 wholebody scans and dosimetry

The administered activity of ^{177}Lu -PSMA617 per cycle was 6.1 ± 0.3 GBq (range 5.4–6.5 GBq) and the total accumulated activity was 18.2 ± 0.9 GBq (range 16.3–19.3 GBq) for 9 patients with 3 cycles and 12.7 ± 0.9 GBq for one patient with 2 cycles.

Dosimetry (Table 2) indicated an average kidney dose of 0.60 ± 0.36 Gy/GBq and an average red bone marrow dose of 0.04 ± 0.03 Gy/GBq. The mean dose to the parotid glands was 0.56 ± 0.25 Gy/GBq, to the sub-mandibular glands, 0.50 ± 0.15 Gy/GBq and to the lacrimal glands, 1.01 ± 0.69 Gy/GBq. Dosimetry data revealed no relevant difference concerning dose values in patients with low or high tumour load. The mean effective dose was 0.08 ± 0.07 Sv/GBq (range 0.02–0.26 Sv/GBq). The accumulated dose for the most sensible organs (kidney, red marrow, salivary and lacrimal

Table 2 Dosimetric calculations of ¹⁷⁷Lu-PSMA617 therapy (Gy/GBq)

Patient	Red marrow	Lacrimal glands	Parotid glands	Sub-mandibular glands	Kidneys	Urinary bladder wall	Osteogenic cells	Spleen	Liver	Small intestine	Gallbladder wall	Pancreas	ULI wall	LLI wall	Effective dose ImSv/M13q)	Skeletal metastases	Lymph node metastases	Visceral metastases
1	0.027	0.680	0.390	0.460	0.674	0.687	0.079	0.089	0.048	0.027	0.028	0.028	0.027	0.028	0.063	1.700	/	/
2	0.024	0.500	0.600	0.460	0.970	0.137	0.060	0.179	0.110	0.025	0.027	0.026	0.025	0.024	0.046	3.680	/	/
3	0.070	0.800	0.250	0.660	1.390	0.127	0.255	0.079	0.256	0.078	0.082	0.081	0.078	0.077	0.117	3.120	/	/
4	0.018	1.100	0.450	0.220	0.319	0.017	0.045	0.186	0.082	0.017	0.019	0.019	0.017	0.017	0.024	2.300	/	/
5	0.074	2.700	0.750	0.650	0.614	0.145	0.128	0.185	0.087	0.342	0.042	0.042	0.044	0.041	0.056	5.510	/	/
6	0.027	0.630	0.850	0.630	0.457	0.149	0.069	0.020	0.119	0.019	0.021	0.020	0.019	0.019	0.041	1.700	2.850	1.700
7	0.096	0.860	0.500	0.580	0.109	0.336	0.411	0.096	/	0.100	0.147	0.117	0.104	0.094	0.264	7.170	/	3.250
8	0.017	1.300	1.040	0.440	0.638	0.127	0.059	0.023	0.125	0.023	0.025	0.024	0.023	0.022	0.046	4.950	/	/
9	0.0453	/	0.420	/	0.372	0.229	0.182	0.061	0.123	0.062	0.063	0.063	0.062	0.062	0.076	1.100	/	2.350
10	0.0246	0.480	0.360	0.380	0.461	0.262	0.083	0.317	0.093	0.030	0.031	0.031	0.030	0.030	0.050	2.800	2.250	/
Min	0.017	0.480	0.250	0.220	0.109	0.017	0.045	0.020	0.048	0.017	0.019	0.019	0.017	0.017	0.024	1.100	2.250	1.700
Mean	0.042	1.006	0.561	0.498	0.600	0.222	0.137	0.123	0.116	0.072	0.048	0.045	0.043	0.041	0.078	3.403	2.550	2.433
Max	0.096	2.700	1.040	0.660	1.390	0.687	0.411	0.317	0.256	0.342	0.147	0.117	0.104	0.094	0.264	7.170	2.850	3.250
Standard deviation	0.028	0.690	0.248	0.146	0.362	0.185	0.117	0.092	0.058	0.099	0.040	0.032	0.029	0.027	0.070	1.940	0.424	0.778

glands) and also for all other organs was remarkably lower compared to malignant lesions. The calculated mean absorbed dose for the tumour lesions ($n = 29$ lesions) averaged for all patients was 2.8 ± 0.5 (range 1.1–7.2) Gy/GBq. For bone metastases, the accumulated dose was 3.40 ± 1.94 Gy/GBq, for LN metastases, 2.55 ± 0.42 Gy/GBq and for visceral lesions, 2.43 ± 0.78 Gy/GBq. Distinct values and additional (not dose-limiting) organs are presented in Table 2.

Response evaluation of $^{177}\text{Lu-PSMA617}$ therapy

To evaluate the response to therapy, we compared the $^{68}\text{Ga-PSMA-HBED-CC}$ PET/CT and $^{177}\text{Lu-PSMA617}$ post-therapy whole-body scans before and after two and three therapy cycles (Table 3). The evaluation of overall therapy response (soft tissues and bone lesions) showed a PR in three patients (Fig. 1), MX in three, SD in one and PD in three patients.

Response to therapy (both $^{68}\text{Ga-PSMA-HBED-CC}$ PET/CT and $^{177}\text{Lu-PSMA617}$ 24-h whole-body scans) was observed already after two therapy cycles. However, this result was not found for all metastases in each patient.

For response evaluation, we analysed the uptake of the tumour lesions in the $^{68}\text{Ga-PSMA-HBED-CC}$ PET (SUV_{max}). We could observe a significant ($p < 0.05$) decrease of SUV_{max} already after 2 treatment cycles in 41/53 skeletal lesions (77.4%), in 12/13 LN metastases (92%), in 3/4 visceral lesions (75%) and in all prostatic lesions (4/4). After 3 cycles 80% (25/31) of skeletal lesions, 88% of LN metastases (8/9), 50% (1/2) of visceral metastases and all 4 prostate lesions showed a significant ($p < 0.05$) decrease. The mean SUV_{max} value of 20.2 for skeletal metastases before therapy decreased to 15.0 after 2 cycles and to 11.5 after 3 therapy cycles.

Additionally, we compared the metabolic and morphological changes seen in $^{68}\text{Ga-PSMA HBED-CC}$ PET/CT with the visual uptake in $^{177}\text{Lu-PSMA617}$ 24-h whole-body scans and found a good correlation in all 10 patients. However, the number of lesions visualized by PET/CT was about 30% higher compared to SPECT/CT.

Seven patients showed a PR, one a MX, one a SD and one showed PD in soft tissue lesions (visceral and LN metastases) after three therapy cycles. Response of skeletal lesions was less pronounced than response of soft tissue lesions: three patients showed a PR, three a MX, one a SD and three a PD.

$^{18}\text{F-NaF}$ PET evaluation showed multiple bone metastases in all patients. Overall, uptake in $^{18}\text{F-NaF}$ PET did not show a noticeable intensity change in the known skeletal lesions during the whole observation period.

Furthermore, changes of PSA levels did not correlate strongly with $^{68}\text{Ga-PSMA-HBED-CC}$ PET/CT results. PSA values significantly declined in two patients with MX response (nos. 2 and 3) and in one patient with PR (no. 7). In patient no. 3, we could observe a rapid progression of metastases in PET/CT accompanied by a simultaneous decrease of

PSA. In patient no. 7, we found an increased PSA despite a reduction of SUV_{max} values in metastatic lesions in $^{68}\text{Ga-PSMA-HBED-CC}$ PET/CT and also improvement of the Karnofsky index (from 70 to 90).

Comparison of absorbed doses and SUV_{max} values

A mean absorbed dose of 59.6 ± 35.2 Gy (range 20.5–135.0) was observed for skeletal metastases correlating to initial SUV_{max} values of 20.2 ± 10.0 (range 8.0–35.7) which decreased to 11.5 ± 6.2 (range 5.4–22.1) after 3 therapy cycles (see Table 4). The mean absorbed dose for LN metastases amounted to 46.5 ± 7.3 Gy (range 41.3–51.6) correlating to a pre-therapeutic SUV_{max} of 15.8 ± 7.0 (range 4.1–21.4) which decreased to 8.6 ± 9.7 (range 1.1–22.5) after 3 therapy cycles. For visceral metastases, the mean absorbed dose was 45.2 ± 15.3 Gy (range 30.8–61.2), which correlated to an initial SUV_{max} value of 23.2 ± 5.9 (range 16.9–28.6) and amounted to 19.7 ± 7.1 (range 14.6–24.7) after 3 therapy cycles.

Safety evaluation

$^{177}\text{Lu-PSMA617}$ therapy was well-tolerated by all patients. In none of the patients were significant adverse effects reported during their hospitalization. No relevant therapy-related side-effects were reported for the bone marrow, liver and kidneys (Table 2). Following therapy, xerostomia was reported in 3/10 patients, which was transient in 2 patients and permanent in 1 patient. Fatigue was observed in 2/10 patients, nausea/loss of appetite in 1/10 patients and constipation also in 1/10 patients. Six out of 10 patients complained about skeletal pain due to the presence of bone metastases. The highest doses were found for the parotid and sub-mandibular glands and a detailed analysis is presented in Table 5. Under the assumption of a constant tracer uptake, after 3 therapy cycles, the mean dose to the parotid glands was 9.4 ± 3.6 Gy (range 4.7–15.4, $n = 10$) corresponding to a mean pre-therapeutic SUV_{max} value of 12.4 ± 6.0 (range 7.5–26, $n = 10$) which amounted to 11.7 ± 4.0 (range 7.0–18.7, $n = 10$) after 3 therapy cycles and resulted in a shrinkage of the gland from 25.0 ± 5.0 ml (range 18.8–34.0, $n = 10$) to 20.0 ± 3.5 ml (range 15.0–26.0, $n = 9$). A similar result was seen for the sub-mandibular glands: the mean absorbed dose was 8.8 ± 3.0 Gy (range 3.6–12.3, $n = 9$) corresponding to an initial SUV_{max} value of 13.4 ± 5.5 (range 7.0–23.2, $n = 10$) which decreased to 12.0 ± 4.2 (range 4.8–18.3, $n = 10$) after 3 therapy cycles. The decline corresponded to a volume reduction from 8.6 ± 1.1 ml (range 7.3–10.4, $n = 10$) to 7.8 ± 1.8 ml (range 6.1–12.0, $n = 10$).

Table 3 Response to treatment with ^{177}Lu -PSMA617 (after 8–10 weeks)

Patient	Accumulated activity GBq	Number of cycles	Therapy-related side effects			Response visceral and lymph node metastases	Response skeletal metastases	PSA before therapy	PSA after therapy	Overall response
			Hematotoxicity (grade)	Hepatotoxicity (grade)	Nephrotoxicity (grade)					
1	17.7	3	I → I	I → I	0	PR	PD	264	531	PD
2	19.3	3	0	I → I	I → I	PR	MX	24.49	3.7	MX
3	18.6	3	I → I	I → I	0	MX	MX	482	92	MX
4	16.3	3	0	0	0	PR	MX	22	21	MX
5	17.9	3	I → I	I → I	0	PR	PR	13.7	7.1	PR
6	18.1	3	0	I → I	0	PR	PR	1338	821.1	PR
7	18.8	3	0	I → I	0	PR	PR	873	2493	PR
8	12.7	2	I → I	I → I	I → II	SD	PD	140	719	PD
9	18.6	3	II → II	II → II	0	PD	PD	119	197	PD
10	18.4	3	0	I → I	0	PR	SD	4.7	3	SD

Discussion

Dosimetry

Different from the application of cytotoxic pharmaceuticals, possible side effects from theragnostics can be estimated by dosimetry which is mandatory in mCRPC patients because of substantial individual variation. Furthermore, there exist well-defined radiation tolerance limits for normal organs.

The main elimination process of ^{177}Lu -PSMA617 occurs via the renal system. Based on EBRT, an absorbed kidney dose limit of 23 Gy has been assumed [28], which probably does not predict renal toxicity from radionuclides. Correction of these data [4] suggested a renal absorbed dose limit of 37 Gy, the biologic effective dose (BED). Assuming a maximal tolerable kidney dose of 37 Gy for radionuclides, on the basis of our dosimetry data with 0.60 ± 0.35 Gy/GBq (range 0.11 to 1.39) for the kidneys, the maximal administrable

Fig. 1 ^{68}Ga -PSMA-HBED-CC PET/CT of patient no. 6 before PET/CT of patient no. 6 before ^{177}Lu -PSMA617 therapy (left), after two (12.1 GBq; middle) and three therapy cycles (18.1 GBq; right). The SUV_{max} value decreased from 27.7 to 20.4 in skeletal metastases, from 37.9 to 23.9 in LN metastases and from 32.3 to 40.5 in liver metastases, whereas SUV_{max} also decreased from 17.8 to 10.4 in the parotid glands and from 23.2 to 14.2 in the sub-mandibular glands

^{68}Ga -PSMA-HBED-CC-PET/CT of patient No. 6

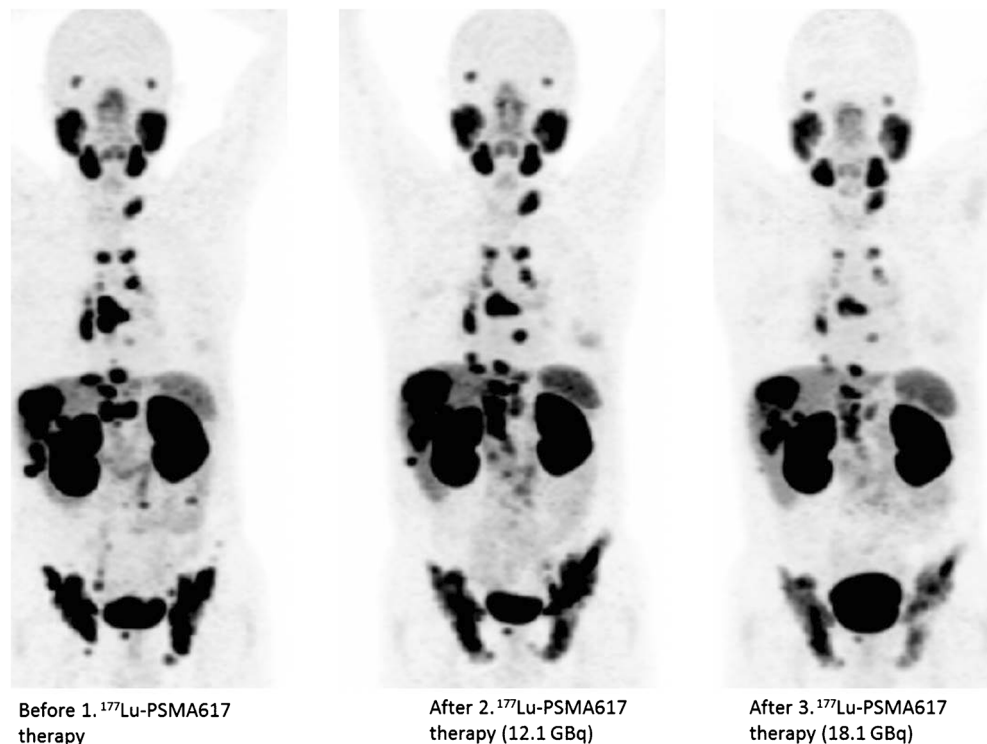


Table 4 Dosimetric calculations of ¹⁷⁷Lu-PSMA617 therapy compared to mean SUV_{max} values

Patient	Therapy cycles	Accumulated activity (GBq)	Skeletal metastases				Lymph node metastases				Visceral metastases						
			Absorbed dose		SUV _{max}		Absorbed dose		SUV _{max}		Absorbed dose		SUV _{max}				
			D/A ^a (Gy/GBq)	D _{tot} ^b (Gy)	Baseline	After two cycles	After three cycles	D/A ^a (Gy/GBq)	D _{tot} ^b (Gy)	Baseline	After two cycles	After three cycles	D/A ^a (Gy/GBq)	D _{tot} ^b (Gy)	Baseline	After two cycles	After three cycles
1	3	17.7	1.70	30.16	12.40	11.98	9.78	/	/	16.50	3.33	7.93	/	/	/	/	/
2	3	19.3	3.68	71.17	21.53	8.40	/	/	/	/	/	/	/	/	/	/	/
3	3	18.6	3.12	58.13	18.12	11.00	11.97	/	/	20.88	4.60	2.95	/	/	/	/	/
4	3	16.3	2.30	37.49	8.00	5.40	5.49	/	/	/	/	/	/	/	/	/	/
5	3	17.9	5.51	98.52	9.60	5.58	5.40	/	/	4.10	1.20	1.10	/	/	/	/	/
6	3	18.1	1.70	30.80	30.37	28.87	22.07	2.85	51.64	16.00	21.80	22.50	1.70	30.80	28.55	34.25	24.70
7	3	18.8	7.17	135.01	27.65	18.83	14.10	/	/	/	/	/	3.25	61.20	16.90	12.20	14.60
8	2	12.7	4.95	62.87	9.99	12.79	/	/	/	/	/	/	/	/	/	/	/
9	3	18.6	1.10	20.45	28.93	15.63	/	/	/	/	/	/	2.35	43.69	24.10	17.75	/
10	3	18.4	2.80	51.41	35.65	31.58	/	2.25	41.31	21.43	12.48	/	/	/	/	/	/
		Mean	3.40	59.60	20.22	15.01	11.47	2.55	46.48	15.78	8.68	8.62	2.43	45.23	23.18	21.40	19.65
		SD	1.94	35.17	10.03	9.05	6.24	0.42	7.31	6.98	8.48	9.69	0.78	15.26	5.88	11.47	7.14
		Minimum	1.10	20.45	8.00	5.40	5.40	2.25	41.31	4.10	1.20	1.10	1.70	30.80	16.90	12.20	14.60
		Maximum	7.17	135.01	35.65	31.58	22.07	2.85	51.64	21.43	21.80	22.50	3.25	61.20	28.55	34.25	24.70
		Max/min	6.52	6.60	4.46	5.85	4.09	1.27	1.25	5.23	18.17	20.45	1.91	1.99	1.69	2.81	1.69

^a Absorbed dose per unit administered activity

^b Total cumulative dose

Table 5 Dosimetric calculations of the salivary glands after ^{177}Lu -PSMA617 therapy (SUV_{max} , volume)

Patient	Therapy cycles	Accumulated activity (GBq)	Parotid glands						Sub-mandibular glands					
			Absorbed dose		Baseline		After three therapy cycles		Absorbed dose		Baseline		After three therapy cycles	
			D/A ^a (Gy/GBq)	D _{tot} ^b (Gy)	SUV _{max}	Volume (ml)	SUV _{max}	Volume (ml)	SUV _{max}	Volume (ml)	D/A ^a (Gy/GBq)	D _{tot} ^b (Gy)	SUV _{max}	Volume (ml)
1	3	17.74	0.39	6.92	26.00	27.00	15.45	21.40	0.46	8.16	19.65	8.65	11.45	8.00
2	3	19.34	0.60	11.60	14.40	29.23	10.55	22.25	0.46	8.90	16.80	7.57	11.35	6.10
3	3	18.63	0.25	4.66	9.35	24.65	8.45	21.00	0.66	12.30	12.45	9.05	13.85	6.85
4	3	16.30	0.45	7.34	10.25	18.75	10.20	14.95	0.22	3.59	10.35	9.40	10.65	9.10
5	3	17.88	0.75	13.41	7.85	25.75	10.05	19.80	0.65	11.62	8.35	7.45	10.25	6.15
6	3	18.12	0.85	15.40	17.80	22.35	10.35	21.50	0.63	11.42	23.15	9.85	14.20	8.20
7	3	18.83	0.50	9.42	14.95	18.90	16.95	15.80	0.58	10.92	17.50	9.30	18.25	8.05
8	2	12.70	1.04	13.21	7.50	34.00	7.00	26.00	0.44	5.59	9.05	7.30	7.45	6.10
9	3	18.59	0.42	7.81	8.05	25.70	8.75	17.30			7.00	7.35	4.75	7.25
10	3	18.36	0.36	6.61	7.80	23.50	18.70		0.38	6.98	9.40	10.35	17.50	11.95
		Mean	0.56	9.64	12.40	24.98	11.65	20.00	0.50	8.83	13.37	8.63	11.97	7.78
		SD	0.25	3.56	5.99	4.59	3.95	3.48	0.15	3.02	5.52	1.13	4.17	1.79
		Minimum	0.25	4.66	7.50	18.75	7.00	14.95	0.22	3.59	7.00	7.30	4.75	6.10
		Maximum	1.04	15.40	26.00	34.00	18.70	26.00	0.66	12.30	23.15	10.35	18.25	11.95
		Max/min	4.16	3.31	3.47	1.81	2.67	1.74	3.00	3.43	3.31	1.42	3.84	1.96

^a Absorbed dose per unit administered activity^b Total cumulative dose

activity would be 61.66 ± 35.97 GBq. In our patient cohort, the administered activity of 18.2 ± 0.9 GBq resulted in a mean kidney dose of 10.66 ± 6.95 Gy (range 2.05 to 25.9, $n = 10$). Thus, on the condition that individual patient dosimetry is performed almost three times higher, activities of ^{177}Lu -PSMA617 may possibly be administered concerning the dose-limiting kidney toxicity. Kabasakal et al. [29] reported an absorbed kidney dose of 0.88 ± 0.40 Gy/GBq for ^{177}Lu -PSMA617 and suggested that a mean activity limit of 30 GBq can safely be applied on the basis of the generally accepted kidney dose of 23 Gy for EBRT. These calculations would suggest that the mean administrable activity for the kidneys lies between 30 and 60 GBq, by large inter-individual variation which indicates once more the need for individual patient dosimetry. Kratochwil et al. [19] also recently suggested that the renal tolerance limit of ^{177}Lu -PSMA617 would permit about twice the administered activity, i.e. 36 GBq. In addition, co-medication of PSMA inhibitors such as 2-(phosphonomethyl) penanedioic acid (PMPA) could improve the kidney to tumour ratio [30], demonstrating future potential. Furthermore, the fractionation regime enables the administration of probably higher activities, in line with previous reports on peptide receptor radionuclide therapy with radiolabeled somatostatin analogues [31], as renal function

may be affected in mCRPC patients due to prior chemotherapy and/or accompanying diseases diabetes and hypertension.

The risk of the development of hematotoxicity is increased in extensively pre-treated mCRPC patients. Especially, patients with extensive bone marrow involvement and previous chemotherapies may respond with higher hematotoxicity. To decrease the probability of severe bone marrow toxicity a threshold of 2 Gy absorbed dose to the red marrow is generally recommended in radionuclide therapy dosimetry [32]. The mean red marrow dose in our patients amounted to 0.042 ± 0.028 Gy/GBq (range 0.017 to 0.096) which resulted in an average absorbed dose of 0.77 ± 0.53 Gy (range 0.21 to 1.81, $n = 10$) suggesting that the tolerable administered activity for the bone marrow should lie around 45 GBq of ^{177}Lu -PSMA617, again, by large individual variation, indicating the importance of pre-therapeutic dosimetry. Kabasakal et al. [29] suggested that even an activity of 65 GBq of ^{177}Lu -PSMA617 is clinically safe for the bone marrow, whereas Ahmadzadehfar et al. [15] reported one grade 3–4 toxicity in 10 patients treated with a mean of only 5.6 GBq. We believe that fractionation of therapy is the best way to avoid severe bone marrow toxicity as published tolerance limits do not seem to be reliable for the concept of receptor-based radionuclide therapies [31].

Comparison of absorbed doses and SUV_{max} values

A high pre-therapeutic SUV_{max} value may serve as a rough indicator for a high absorbed dose and, thus, better clinical response. In order to determine a possible relation between SUV_{max} values from PET/CT and absorbed dose values at the subsequent therapy, SUV_{max} values and the corresponding absorbed dose of organs and tumours have been evaluated (Table 4). A correct mapping of the organ or tumour in the two different imaging modalities (PET/CT and whole-body imaging from dosimetry measurements) was crucial. Due to aberrations between these two imaging modalities and missing SPECT imaging for 3D volume evaluation, the mapping was not successful in each case. Furthermore, for local relapse in the prostate bed, it was difficult to determine the correct correlation between SUV_{max} value and absorbed dose due to overlap of the bladder activity. While Baum et al. [13] reported that the median SUV_{max} value decreased significantly in lesions with higher absorbed doses, we could not find a significant correlation of SUV_{max} values and absorbed dose estimates in our patients. Kratochwil et al. [30] also found 50% decreased SUV_{max} values but no attempt to correlate them with absorbed dose calculation was made. In line with our data, in a very recent study, Okamoto et al. [33] also report only moderate correlation of pre-therapeutic SUVs with absorbed dose estimates using a PSMA inhibitor for imaging and therapy (PSMA I&T). Obviously, besides target expression, also other factors of tumour biology are present which determine therapy response. This observation and the advent of novel PSMA ligands for potential therapy selection, in particular ^{18}F ligands [34, 35], call for more prospective clinical studies to provide the optimal tools for selection of patients, which may benefit most from targeted radionuclide therapy with PSMA ligands.

Response evaluation of ^{177}Lu -PSMA617 therapy

RECIST criteria

The results of our study support recent reports that ^{177}Lu -PSMA617 radionuclide therapy can be an effective treatment modality when all other available treatment options have failed. In our patients, response to therapy as measured by ^{68}Ga -PSMA-HBED-CC PET/CT and ^{177}Lu -PSMA617 whole-body scanning was obtained in 7 of 10 patients (response rate 70%) who showed either a PR ($n=3$) or MX ($n=3$), or who had a SD ($n=1$) at 9 weeks after 3 therapy cycles of ^{177}Lu -PSMA617 with a mean absorbed dose of 2.8 ± 0.52 Gy/GBq of the tumour lesions ($n=29$). Despite minimal toxicity in all patients, four patients are still alive at 8 months after completion of ^{177}Lu -PSMA617 therapy.

The potential of the $^{68}Ga/^{177}Lu$ theragnostic concept was first proven using the ligands DOTAGA-(l-y)fk(Sub-KuE),

also named PSMA I&T [14], and PSMA617 [36]. Using ^{177}Lu -PSMA I&T, Baum et al. [13] recently reported for 25 patients who had more than 2 therapy cycles (up to 6 cycles) a PR in 14, SD in 2, PD in 9 patients (response rate 64%), but no “mixed responses” were observed by ^{68}Ga -PSMA-HBED-CC PET/CT. The authors point out that dual-phase CT gave different results from ^{68}Ga -PSMA-HBED-CC PET/CT with PR in 5, SD in 13 and PD in 7 patients, a discrepant finding discussed on the lower sensitivity of the stand-alone CT compared to PET in the assessment of skeletal metastases and small LN metastases. In our point of view, these diverging results reflect also the high rate of “mixed responses” seen in 3 of our 10 patients who developed new lesions at one metastatic site, whereas they responded remarkably at another lesion site. Even with lower accumulated activities (2 cycles, 3.7–6 GBq/cycle) of ^{177}Lu -PSMA617, Fendler et al. [37] reported a PR in 4 patients and SD in 6/15 patients which results in a response rate of 67%.

It can be assumed that the strong tumour response in roughly 2/3 of patients is attributable to the high doses delivered to the tumours. In our study, the mean tumour dose amounted to 2.8 ± 0.53 Gy/GBq (range 1.1 to 7.2 Gy/GBq, $n=29$). Kratochwil et al. [19] reported a tumour dose range between 6 and 22 Gy/GBq for ^{177}Lu -PSMA617 and Baum et al. [13] reported a tumour dose range of 0.03 and 78 (median 3.3) Gy/GBq for ^{177}Lu -PSMA I&T. The highest absorbed tumour dose (468 Gy) ever reported was found for a para-aortic LN which exhibited an SUV_{max} value of 187.5 [13]. Using 3D SPECT dosimetry, Delker et al. [17] recently reported absorbed doses for tumour lesions ranging between 1.2 and 47.5 Gy (13.1 Gy/GBq). In our cohort, the highest pre-therapeutic SUV_{max} value was 74.4 corresponding to a skeletal metastasis.

PSA level

Using PSA as a response parameter, Kratochwil et al. [19] found in 8 of 11 patients who were treated with 3 cycles of ^{177}Lu -PSMA617 a sustained PSA response (>50%) for over 24 weeks which correlated to radiological response. PSA response can be seen as early as after one therapy cycle only with a decline of more than 50% from baseline values [15]. In 47/74 patients (64%), a PSA decline was noticed after 1 therapy cycle only (5.9 ± 0.5 GBq) with a pronounced decline of >50% in 23 (i.e. 31%) patients [18]. Similar response with a PSA decline >50% in about 60% of patients was reported by Baum et al. [13] for an inhomogeneous group receiving up to 5 cycles of ^{177}Lu -PSMA I&T. In our group of 10 consecutive patients, PSA response was found in 5 patients (50%), who also showed an objective radiological and metabolic response by ^{68}Ga -PSMA-HBED-CC PET/CT in terms of PR, MX or SD. In accordance with the findings of Kratochwil et al. [19]

and Yadav et al. [38], we also found diverging results of PSA levels and PET/CT as well as whole-body imaging.

¹⁸F-NaF PET imaging

In our series of patients, ¹⁸F-NaF PET scans did not change over the observation period and did not add additional information to the treatment outcome. ¹⁸F-NaF PET is representing skeletal metabolism and its uptake proves not only the presence of vital tumor cells in osteoblastic metastases but also shows an increased bone metabolism in necrotic areas, induced by bisphosphonate therapy, in sclerotic processes as a sign of bone remodeling after successful cancer treatment, including efficient androgen deprivation therapy, and/or fractures as well as in degenerative and inflammatory bone diseases [39, 40]. Especially in highly dense sclerotic lesions, ⁶⁸Ga-PSMA-HBED-CC PET/CT as well as ¹⁸F-NaF PET/CT might, therefore, have negative results.

The unspecific sclerotic processes partially explain the mismatch between the subjective pain relief accompanied by an improvement in the ⁶⁸Ga-PSMA-HBED-CC PET/CT and no significant intensity changes in the bone scintigraphy following ¹⁷⁷Lu-PSMA617 therapy.

Because of the low specificity, ¹⁸F-NaF PET/CT is not suitable for response evaluation of ¹⁷⁷Lu-PSMA617 therapy. Imaging reflecting bone remodeling is, however, recommended for treatment planning purposes, especially in patients with clinical suspicion of bone involvement [40].

Side effects

In none of our patients were relevant therapy-related side effects observed using a mean accumulated dose of 18.2 ± 0.9 GBq. It has to be mentioned that all our patients already had undergone extensive pre-treatments and had PD before receiving ¹⁷⁷Lu-PSMA617 therapy as an ultimate treatment option (Table 1).

The PSMA-targeting molecule, MIP-1095, which was first used for therapy in mCRPC patients, was labeled with ¹³¹I, proving the ¹²⁴/¹³¹I theragnostic concept [4]. This molecule, however, led to significant xerostomia and mucositis probably due to long retention of the radionuclide in the glands. Only in one of our patients (no. 5), did we observe a permanent xerostomia after 3 therapy cycles with an absorbed dose of 13.4 Gy to the parotid glands and 11.6 Gy to the submandibular glands, and in this patient, the volume of the glands decreased from 25.8 to 19.8 ml and from 7.5 to 6.2 ml, respectively. In general, ¹⁷⁷Lu-PSMA617 therapy led to significantly decreased SUV_{max} values accompanied by volume reduction ($p < 0.05$). Salivary gland damage is a frequent side effect of EBRT [41] as well as ¹³¹I radioablation therapy of thyroid cancer [42] and may impair the quality of life. Dysfunction is usually transient [43] and a maximal dose

limit of 45 Gy has been suggested with a dose of 30 Gy for total recovery within 2 years [41]. Assuming a dose of 0.5 ± 0.15 Gy/GBq for the salivary glands, the mean absorbed dose amounts to around 9 Gy for an activity of 18 GBq in our patients suggesting that an activity of 60 GBq of ¹⁷⁷Lu-PSMA617 can be administered, by large variation.

Limitations

The main limitation of this report in mCRPC is that our cohort was already suffering from a very advanced disease stage with negative prognostic factors such as Gleason score, visceral metastases and extensive pre-treatments. This may be seen as a negative referral bias. Results may be better in patients with a more confined disease extent and fewer pre-treatments. Treatment stratification was based on PET/CT positivity and disease progression, thereby tailoring selection for radionuclide therapy. Decreasing SUV_{max} values and volumes have been found for many tumour lesions (but not all), but also for normal organs (salivary glands) which must be considered as higher doses could be used in a future tumour control strategy. Finally, definition of response to therapy also is a problem. Only a combination of available measures (clinical status, quality of life measurements, PSA values, PET/CT with PSMA ligands, CT, MR) seems to be appropriate; the most important one probably remains the clinical status of the mostly elderly patient.

Conclusion

Due to substantial individual variance, dosimetry is mandatory for a patient-specific approach to prevent organ toxicity. Our dosimetry data suggest that higher activities and/or shorter treatment intervals should be applied in a larger prospective study.

Acknowledgements Open access funding provided by University of Innsbruck and Medical University of Innsbruck. The authors express gratitude to Drs. Geraldo-Roig L., Kroiss A., Nilica B., Mair C., Warwitz B., von Guggenberg E. and Haubner R., and to the nursing staff and nuclear technologists of the Department of Nuclear Medicine at the Medical University of Innsbruck. We express our gratitude to Meister A. for helping to prepare the manuscript.

Compliance with ethical standards

Conflicts of interest The authors declare that they have no conflicts of interest.

Research involving human participants and/or animals The application of ¹⁷⁷Lu-PSMA617 was approved by the institutional review tumour board and all patients gave written informed consent to therapy and imaging studies. All patients received ¹⁷⁷Lu-PSMA617 under compassionate use condition according to the updated Declaration of Helsinki [22], prepared according to the Austrian Medicinal Products Act, AMG §

8a [23]. All patients were informed about the experimental nature of the ^{177}Lu -PSMA617 therapy and no systematic patient selection was performed. All regulations of the Austrian Agency for Radiation Protection were observed [24].

Informed consent According to the Austrian laws, for this type of study, a formal consent is not required.

Open Access This article is distributed under the terms of the Creative Commons Attribution 4.0 International License (<http://creativecommons.org/licenses/by/4.0/>), which permits unrestricted use, distribution, and reproduction in any medium, provided you give appropriate credit to the original author(s) and the source, provide a link to the Creative Commons license, and indicate if changes were made.

References

- National Cancer Institute, Surveillance Epidemiology and End Results, SEER stat fact sheets: prostate. Available from:<http://seer.cancer.gov/statfacts/html/prost.html>.
- Khuntia D, Reddy CA, Mahadevan A, et al. Recurrence free survival rates after external-beam radiotherapy for patients with clinical T1-T3 prostate carcinoma in the prostate specific antigen era: what should we expect? *Cancer*. 2004;100:1283–92.
- Vallabhajosula A, Goldsmith SJ, Hamacher KA, et al. Prediction of myelotoxicity based on bone marrow radiation absorbed dose: radioimmunotherapy studies using ^{90}Y - and ^{177}Lu -labeled J591 antibodies specific for prostate specific membrane antigen. *J Nucl Med*. 2005;46:850–8.
- Zechmann CM, Afshar-Oromieh A, Armor T, et al. Radiation dosimetry and first therapy results with a $^{124}\text{I}/^{131}\text{I}$ -labeled small molecule (MIP-1095) targeting PSMA for prostate cancer therapy. *Eur J Nucl Med Mol Imaging*. 2014;41:1280–92.
- Vallabhajosula S, Nikolopoulou A, Babich JW, et al. $^{99\text{m}}\text{Tc}$ -labeled small-molecule inhibitors of prostate-specific membrane antigen: pharmacokinetics and biodistribution studies in healthy subjects and patients with metastatic prostate cancer. *SJ2. J Nucl Med*. 2014;55:1791–8.
- Ceci F, Uprimny C, Nilica B, et al. ^{68}Ga -PSMA PET/CT for restaging recurrent prostate cancer: which factors are associated with PET/CT detection rate? *Eur J Nucl Med Mol Imaging*. 2015;42:1284–94.
- Sterzing F, Kratochwil C, Fiedler H, et al. ^{68}Ga -PSMA-11 PET/CT: a new technique with high potential for the radiotherapeutic management of prostate cancer patients. *Eur J Nucl Med Mol Imaging*. 2016;43:34–41.
- Chatalic KL, Heskamp S, Konijnenberg M, et al. Towards personalized treatment of prostate cancer: PSMA I&T, a promising prostate-specific membrane antigen-targeted theranostic agent. *Theranostics*. 2016;6:849–61.
- Morigi JJ, Stricker PD, van Leeuwen PJ, et al. Prospective comparison of ^{18}F -Fluoromethylcholine versus ^{68}Ga -PSMA PET/CT in prostate cancer patients who have rising PSA after curative treatment and are being considered for targeted therapy. *J Nucl Med*. 2015;56:1185–90.
- Uprimny C, Kroiss A, Nilica B, et al. ^{68}Ga -PSMA ligand PET versus ^{18}F -NaF PET: evaluation of response to ^{223}Ra therapy in a prostate cancer patient. *Eur J Nucl Med Mol Imaging*. 2015;42:362–3.
- Gillessen S, Omlin A, Attard G. Management of patients with advanced prostate cancer: recommendations of the St Gallen Advanced Prostate Cancer Consensus Conference (APCCC). *Ann Oncol*. 2015;26:1589–604.
- Maffioli L, Florimonte L, Costa DC, et al. New radiopharmaceutical agents for the treatment of castration resistant prostate cancer. *Q J Nucl Med Mol Imaging*. 2015;59:420–38.
- Baum RP, Kulkarni HR, Schuchardt C, et al. Lutetium-177 PSMA radioligand therapy of metastatic castration-resistant prostate cancer: safety and efficacy. *J Nucl Med*. 2016;57:1006–13.
- Weinisen M, Schottelius M, Simecek J, et al. ^{68}Ga - and ^{177}Lu -Labeled PSMA I&T: optimization of a PSMA-targeted theranostic concept and first proof-of-concept human studies. *J Nucl Med*. 2015;56:1169–76.
- Ahmadzadehfar H, Eppard E, Kürpig S, Fimmers R, Yordanova A, Schlenkhoff CD, et al. Therapeutic response and side effects of repeated radioligand therapy with ^{177}Lu -PSMA-DKFZ-617 of castrate-resistant metastatic prostate cancer. *Oncotarget*. 2016;7:12477–88.
- Afshar-Oromieh A, Hetzheim H, Kratochwil C, et al. The theranostic PSMA ligand PSMA-617 in the diagnosis of prostate cancer by PET/CT: biodistribution in humans, radiation dosimetry, and first evaluation of tumour lesions. *J Nucl Med*. 2015;56:1697–705.
- Delker A, Fendler WP, Kratochwil C, et al. Dosimetry for ^{177}Lu -DKFZ-PSMA-617: a new radiopharmaceutical for the treatment of metastatic prostate cancer. *Eur J Nucl Med Mol Imaging*. 2016;43:42–51.
- Rahbar K, Schmidt M, Heinzel A, et al. Response and tolerability of a single dose of ^{177}Lu -PSMA-617 in patients with metastatic castration-resistant prostate cancer: a multicenter retrospective analysis. *Nuklearmedizin*. 2016;55:123–8.
- Kratochwil C, Giesel FL, Stefanova M, et al. PSMA-targeted radionuclide therapy of metastatic castration-resistant prostate cancer with ^{177}Lu -labeled PSMA-617. *J Nucl Med*. 2016;57:1170–6.
- Kiess AP, Minn I, Chen Y, et al. Auger radiopharmaceutical therapy targeting prostate-specific membrane antigen. *J Nucl Med*. 2015;56:1401–7.
- Kiess A, Minn IL, Vaidyanathan G, et al. (2S)-2-(3-(1-Carboxy-5-(4- ^{211}At -astatobenzamido)pentyl)ureido)-pentanedioic acid for PSMA-Targeted α -Particle Radiopharmaceutical Therapy. *J Nucl Med*. 2016.
- World Medical Association Declaration of Helsinki: ethical principles for medical research involving human subjects. *JAMA*. 2000;284:3043–45.
- Arzneimittelgesetz, BGBI. Nr. 185/1983, last revision BGBI. II Nr. 105/2015, <https://www.ris.bka.gv.at/GeltendeFassung.wxe?Abfrage=Bundesnormen&Gesetzesnummer=10010441>. Updated August 2nd 2016.
- Österreichischer Verband für Strahlenschutz. Mitgliedsgesellschaft der International Radiation Protection Association. <http://www.strahlenschutzverband.at/index.php?id=strahlenschutzrecht0>. Updated July 7, 2016.
- Petrik M, Knetsch PA, Knopp R, et al. Radiolabelling of peptides for PET, SPECT and therapeutic applications using a fully automated disposable cassette system. *Nucl Med Commun*. 2011;32:887–95.
- Common Terminology Criteria for Adverse Events 3.0 (NIH/NCI). http://ctep.cancer.gov/protocolDevelopment/electronic_application/docs/ctcae3.pdf. Accessed 1 Feb 2016.
- Stabin MG, Sparks RB, Crowe E. OLINDA/EXM: the second-generation personal computer software for internal dose assessment in nuclear medicine. *J Nucl Med*. 2005;46:1023–7.
- Emami B, Lyman J, Brown A, et al. Tolerance of normal tissue to therapeutic irradiation. *Int J Radiat Oncol Biol Phys*. 1991;21:109–22.
- Kabasakal L, AbuQbeith M, Aygün A, et al. Pre-therapeutic dosimetry of normal organs and tissues of ^{177}Lu -PSMA-617 prostate-

- specific membrane antigen (PSMA) inhibitor in patients with castration-resistant prostate cancer. *Eur J Nucl Med Mol Imaging*. 2015;42:1976–83.
30. Kratochwil C, Giesel FL, Leotta K, et al. PMPA for nephroprotection in PSMA-targeted radionuclide therapy of prostate cancer. *J Nucl Med*. 2015;56:293–8.
 31. Bodei L, Kidd M, Paganelli G, et al. Long-term tolerability of PRRT in 807 patients with neuroendocrine tumours: the value and limitations of clinical factors. *Eur J Nucl Med Mol Imaging*. 2015;42:5–19.
 32. O'Donoghue JA, Baidoo N, Deland D, et al. Hematologic toxicity in radioimmunotherapy: dose–response relationships for I-131 labeled antibody therapy. *Cancer Biother Radiopharm*. 2002;17:435–43.
 33. Okamoto S, Thieme A, Allmann J, D'Alessandria C, Maurer T, Retz M, et al. Radiation dosimetry for ^{177}Lu -PSMA-I&T in metastatic castration-resistant prostate cancer: Absorbed dose in normal organs and tumor lesions. *J Nucl Med*. 2016.
 34. Giesel FL, Hadaschik B, Cardinale J, Radtke J, Vinsensia M, Lehnert W, et al. F-18 labelled PSMA-1007: biodistribution, radiation dosimetry and histopathological validation of tumor lesions in prostate cancer patients. *Eur J Nucl Med Mol Imaging*. 2016.
 35. Kelly J, Amor-Coarasa A, Nikolopoulou A, Kim D, Williams C Jr, Ponnala S, et al. Synthesis and pre-clinical evaluation of a new class of high-affinity ^{18}F -labeled PSMA ligands for detection of prostate cancer by PET imaging. *Eur J Nucl Med Mol Imaging*. 2016.
 36. Kratochwil C, Giesel FL, Eder M, et al. ^{177}Lu -labelled PSMA ligand-induced remission in a patient with metastatic prostate cancer. *Eur J Nucl Med Mol Imaging*. 2015;42:987–8.
 37. Fendler WP, Reinhardt S, Ilhan H, Delker A, Böning G, Gildehaus FJ, et al. Preliminary experience with dosimetry, response and patient reported outcome after ^{177}Lu -PSMA-617 therapy for metastatic castration-resistant prostate cancer. *Oncotarget*. 2016.
 38. Yadav MP, Ballal S, Tripathi M, Damle NA, Sahoo RK, Seth A, et al. ^{177}Lu -DKFZ-PSMA-617 therapy in metastatic castration resistant prostate cancer: safety, efficacy, and quality of life assessment. *Eur J Nucl Med Mol Imaging*. 2016.
 39. Beheshti M et al. Evaluation of Prostate Cancer Bone Metastases with ^{18}F -NaF and ^{18}F -Fluorocholine PET/CT". *J Nucl Med*. 2016;57:55S–60.
 40. Amzalag G. et al. "Target definition in salvage radiotherapy for recurrent prostate cancer: the role of advanced molecular imaging". Mini review. *Front Oncol*. 2016; Vol. 6 Article 73.
 41. Li Y, Taylor JMG, Ten Haken RK, et al. The impact of dose on parotid salivary recovery in head and neck cancer patients treated with radiation therapy. *Int J Radiat Oncol Biol Phys*. 2007;67:660–9.
 42. Jeong SY, Kim HW, Lee S-W, et al. Salivary gland function 5 years after radioactive iodine ablation in patients with differentiated thyroid cancer: direct comparison of pre- and postablation scintigraphies and their relation to xerostomia symptoms. *Thyroid*. 2013;23: 609–16.
 43. Grewal RK, Larson SM, Pentlow CE, et al. Salivary gland side effects commonly develop several weeks after initial radioactive iodine ablation. *J Nucl Med*. 2009;50:1605–10.